chemosensors

MDPI

Article

Pd-GaSe and Pd_3-GaSe Monolayers: Two Promising Candidates for Detecting Dissolved Gases in Transformer Oil

Tianyu Hou [1], Wen Zeng [2,*] and Qu Zhou [1,*]

[1] College of Engineering and Technology, Southwest University, Chongqing 400715, China; houtianyu_luck@163.com
[2] College of Materials Science and Engineering, Chongqing University, Chongqing 400044, China
* Correspondence: wenzeng@cqu.edu.cn (W.Z.); zhouqu@swu.edu.cn (Q.Z.); Tel.: +86-130-683-05845 (Q.Z.)

Abstract: In this paper, the adsorption behaviors of three gases (H_2, CO, and C_2H_2) decomposed by the transformer oil on Pd-GaSe and Pd_3-GaSe monolayers were calculated by density functional theory. Compared with Pd single-atom doping, Pd_3 cluster doping changed the original structure and charge distribution to a greater extent, and more obviously improved the conductivity. According to the analysis of adsorption energy, charge transfer and deformation charge density, the results show that the two doped structures have better adsorption performance for the three gas molecules (H_2, CO, and C_2H_2) than the intrinsic GaSe monolayer. Compared with Pd-GaSe, Pd_3-GaSe showed stronger adsorption property for the three gases. Analysis of frontier molecular orbitals and recovery characteristics shows that Pd_3-GaSe can be used as an ideal gas sensitive material for H_2 detection because of its good desorption properties and obvious conductivity changes. Pd-GaSe can be used as a disposable resistive sensor for CO. Pd_3-GaSe is a kind of sensing material suitable for disposable resistance sensors for CO and C_2H_2. These two doped structures have great application potential in gas adsorption and detection, and provide indications for further study on gas sensor detection by means of metal-doped GaSe monolayer.

Keywords: Pd-GaSe monolayer; Pd_3-GaSe monolayer; density functional theory; oil-dissolved gases

check for updates

Citation: Hou, T.; Zeng, W.; Zhou, Q. Pd-GaSe and Pd_3-GaSe Monolayers: Two Promising Candidates for Detecting Dissolved Gases in Transformer Oil. *Chemosensors* **2022**, *10*, 236. https://doi.org/10.3390/chemosensors10070236

Academic Editor: Eleonora Alfinito

Received: 18 May 2022
Accepted: 15 June 2022
Published: 21 June 2022

Publisher's Note: MDPI stays neutral with regard to jurisdictional claims in published maps and institutional affiliations.

Copyright: © 2022 by the authors. Licensee MDPI, Basel, Switzerland. This article is an open access article distributed under the terms and conditions of the Creative Commons Attribution (CC BY) license (https://creativecommons.org/licenses/by/4.0/).

1. Introduction

The stability and reliability of power systems play a vital role in the prosperity of any country and the happiness of its people. Therefore, performance requirements for power network equipment are subject to gradual improvement. Power transformers are a crucial and expensive power network equipment necessary for voltage conversion [1–4]. Among them, oil-immersed transformers account for about 90%. Over the long-term operation of the equipment, insulation oil is decomposed into H_2, CO, C_2H_2, and other gases due to insulation overheating, low energy spark, arc, partial discharge, and other faults [5]. Dissolved gas analysis (DGA) is commonly used to diagnose transformer faults because it provides great information about thermal anomalies and electricity [6]. Therefore, early detection of equipment faults helps reduce the losses caused by these faults.

Recently, with the successful research and development of graphene materials, two-dimensional (2D) materials have been broadly studied and successfully applied in many areas such as energy storage and transformation, electronics, and sensing materials due to their unique molecular structure and physicochemical properties [7–12]. In addition, many two-dimensional materials are used for gas sensor detection of dissolved gas in transformer oil in the field of dissolved gas analysis (DGA). By detecting the type and proportion of dissolved gas in transformer oil, we can assess the operation of electrical equipment, analyze the fault type, and then determine the corresponding maintenance method to reduce the loss, which is a significant topic in electric power research in recent times [13–16]. For instance, Qian et al. found that an Au-doped MoS_2 monolayer can

remarkably improve the adsorption performance for C_2H_6 and C_2H_4 gases [17]. At present, the requirement of characteristic gas detection is gradually increasing, and various gas sensors are in the research stage. Two-dimensional materials such as metal oxides, transition metal dihalogens (TMDs), metal nitrides, and carbides have attracted extensive attention in the academic world [18–20]. It is a promising research direction for the study and design of a gas sensor with better performance to detect the characteristic gases.

GaSe is a kind of metal-chalcogen compound with a layered hexagonal structure, belonging to a layered III–VI semiconductor and has been studied since last century. Hu et al. prepared two-dimensional nanosheets of ultrathin GaSe by using mechanical cleavage and solvent exfoliation method [21]. Due to its good ON/OFF ratio, electron differential mobility, low energy of formation and second-order nonlinearity, GaSe has shown wide application prospects in the fields of transistors, water splitting photocatalysts, and nonlinear optics [22–24]. Zhou et al. studied the adsorption performance of monolayer GaSe on several small molecule gases such as H_2, O_2, NO_2, and H_2O, and found that monolayer GaSe has a wide application prospect as O_2 and NO_2 sensors [25]. Increasing research has found that the doping of transition metal (TM) can improve the charge transfer rate between gas and material, thus greatly improving the sensitivity of gas molecules [26–28]. Jiang et al. found that V-GaSe monolayer had higher conductivity and better gas adsorption performance than an intrinsic GaSe monolayer, and could better adsorb SF_6 decomposition products [29]. Among TM atoms, Pd atom, as a doped atom, has significantly enhanced the adsorption performance of the substrate to characteristic gases in many materials doping studies. Cui et al. found that Pd-doped $HfSe_2$ has good adsorption performance for NO_2 and SO_2 molecules [30–32]. At present, there is little research on Pd atom-doped GaSe gas sensitive materials. In this paper, Pd atom-doped GaSe materials for several gases were studied.

To the present time, only few studies have investigated the influence of cluster doping on gas adsorption performance. For example, Gao et al. studied the effect of Ni_n (n = 1, 2, 3, and 4) doped graphene on NO adsorption, and found that the more Ni atoms, the more obvious the effect of Ni on NO adsorption [33]. Cui et al. have studied the structure and electronic characteristics of Rh_n (n = 1–4) cluster doped MoS_2 monolayer, and found that Rh_3-MoS_2 has the best stability and the best electronic behavior [34]. For the above reasons, the Pd_3 cluster doping method is adopted in this paper. Therefore, this paper studies the adsorption behavior of Pd monatomic doped GaSe molecules and Pd_3 cluster-doped GaSe molecules on dissolved gases in transformer oil, and compares the adsorption performance of the two materials.

2. Computation Methods

In this study, all microscopic calculations based on density functional theory (DFT) were performed in $Dmol^3$ module of Materials Studio (MS). For dealing with the electron exchange correlation function and correlation energy, we use the Perdew–Burke–Ernzerhof (PBE) function to calculate the generalized gradient approximation (GGA) [35,36]. We used the Tkatchenko and Schefflfler (TS) method to correct the weak van der Waals forces between the gas molecules and the monolayer material [37]. The DFT-D method was used to calculate the weak interaction between adsorbed atom and substrate to obtain a more accurate result. The DFT semi-core pseudopotential (DSPP) method was used to deal with core electron relativity effects [38]. The double numerical plus polarization (DNP) method was selected for the linear combination of atomic orbitals [39,40]. GaSe supermonomer was constructed for atomic doping and gas adsorption, and was designed to be 14.972 Å × 14.972 Å × 24.7757 Å. To avoid interactions between adjacent cells, the vacuum region of a GaSe supercell was set to 20 Å vertically [41]. A 4 × 4 × 1 Monkhorst-Pack of k-point was used to analyze the Brillouin zones for geometric optimization and electronic structure calculation [42]. Electron spin is unrestricted [29,43,44]. The value of convergence criteria for the energy, maximum force and displacement were severally set as 1×10^{-5} Ha, 2×10^{-3} Ha/Å, and 5×10^{-3} Å.

By calculating binding energy (E_b), the most stable doping structure can be determined. When n is equal to 1 or 3, the binding energy formula of Pd_n doping GaSe is defined as: [45]

$$E_b = E_{Pd_n-GaSe} - E_{GaSe} - n \cdot E_{Pd} \quad (1)$$

where, $E_{Pdn-GaSe}$ and E_{GaSe} are the total energy of Pd_n-doped GaSe and the total energy of GaSe molecular layer respectively. E_{Pd} is the energy of a single Pd atom, when n is equal to 3, 3 E_{Pd} represents the energies of the three isolated Pd atoms [46].

When the gas molecules approach the sensor surface in different ways, the adsorption energy (E_{ad}) is used to characterize the adsorption performance of the material to a single gas molecule [47].

$$E_{ad} = E_{Pd_n-GaSe/gas} - \left(E_{Pd_n-GaSe} + E_{gas}\right) \quad (2)$$

In the above formula, $E_{Pdn-GaSe/gas}$ represents the total energy of the gas adsorption system, E_{gas} represents the total energy of the gas molecule [48]. A larger absolute value of E_{ad} means that the system is more stable [49]. If the absolute value of E_{ad} is less than 0.6 eV, it indicates that the adsorption process is physical adsorption, while when the absolute value of E_{ad} is greater than 0.8 eV, it indicates that chemical adsorption exists in the process [50–52].

We use Muliken charge analysis to calculate the charge transfer between the gases and the Pd_n-GaSe, represented by Q_T.

$$Q_T = Q_{after} - Q_{before} \quad (3)$$

Q_{after} means the charge of the gas molecules after the system absorbs the gases, and Q_{before} represents the charge of the gas molecules before the system absorbs the gases. When Q_T is a positive value, it means that in the adsorption process, the gas loses electrons, and electrons with a value corresponding to $|Q_T|$ are transferred from the gas molecules to the adsorption material. On the contrary, when Q_T is negative, gas acts as an electron acceptor, accepting electrons transferred from the crystal surface [53].

3. Results and Discussion

3.1. Structures of Characteristic Gases, Pd-GaSe, and Pd_3-GaSe Monolayers

Figures 1 and 2 show the optimized dissolved gas molecular structures in transformer oil and the optimized GaSe monolayer, respectively. The H_2 molecule and C_2H_2 molecule have a symmetrical structure. The length of H–H bond in H_2 is 0.749 Å and the length of C–O bond in CO is 1.142 Å. The C–C and C–H bonds in C_2H_2 molecule are 1.211 Å and 1.071 Å in length, separately. The optimized data of gas molecular structures are the same as the experimental results of previous research [54,55]. Figure 2 shows the top and side views of the intrinsic GaSe, where the Ga–Se bond length is 2.472 Å. GaSe belongs to two-dimensional network structure.

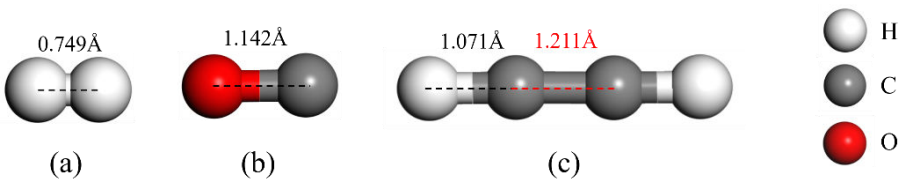


Figure 1. Structures of (**a**) H_2, (**b**) CO, and (**c**) C_2H_2.

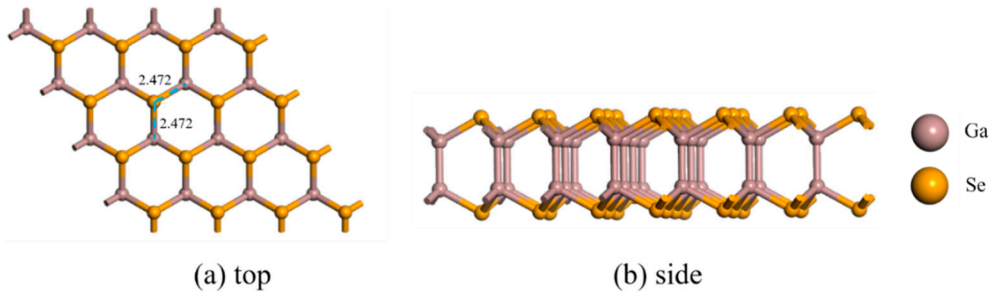


Figure 2. Geometric model of GaSe monolayer.

Firstly, Pd single-doped GaSe was studied. There were three possible doping positions considered, namely T_H (hexagonal ring center of GaSe), T_{Ga} (top of Ga atom), T_{Se} (top of Se atom), and T_B (bridge site between two Se atoms) [30]. The configurations of the four doping sites were optimized, and the binding energies of the four models were calculated as −2.214 eV, −2.316 eV, −1.901 eV and −2.170 eV, respectively. The more negative E_b is, the better the stability is, it corresponds to the most ideal doping site. Therefore, T_{Ga} was selected as the doping site for subsequent research. Figure 3 shows its structure. The TDOS and PDOS diagrams of Pd-doped system are given in Figure 4. One can see that the TDOS of the Pd-GaSe system moves to the lower energy level as a whole, and the intercept at Fermi level decreases. Therefore, this shows that doping of Pd reduces the energy band of GaSe. The decrease of energy band indicates that the transition of electrons becomes easier, so the conductivity of the system is enhanced [56]. It can be seen from PDOS in Figure 4b that Pd-4d orbital overlaps with Se-4p orbital near −2.7 eV, indicating that a chemical bond between Pd and Se is formed, thus changing the charge distribution of the system. The results show that Pd and Se interact with each other.

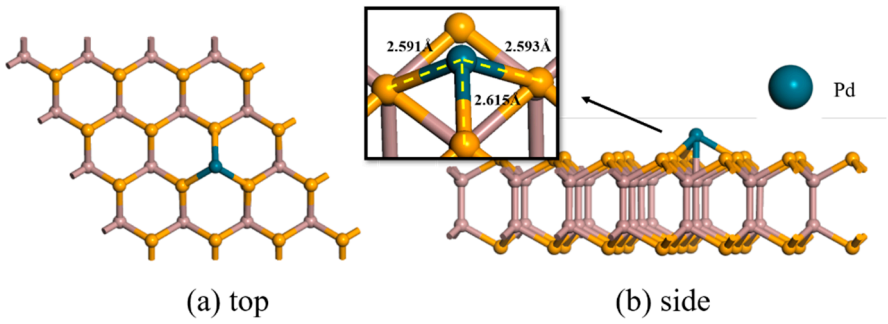


Figure 3. Geometric model of the Pd-GaSe monolayer.

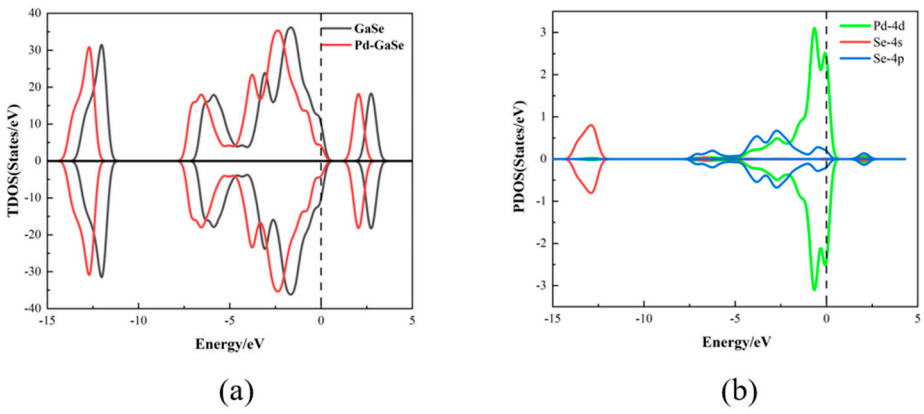


Figure 4. (**a**) TDOS of GaSe monolayer, Pd-GaSe monolayer, (**b**) PDOS of Pd-GaSe monolayer.

Secondly, the Pd_3-GaSe system was analyzed. Three common doping sites were considered in this paper, [19] and two relatively stable models were obtained by optimizing the established model without serious distortion, as illustrated in the Figure 5. The optimized binding energies of the two structures are −6.616 eV and −6.627 eV severally. Similarly, a larger absolute value of binding energy means that the structure is more stable. Therefore, the model B is selected for subsequent research. Bonds are formed between Pd and Se atoms, and the three Pd atoms form an approximate equilateral triangle with 2.932 Å, 2.910 Å and 2.842 Å in bond length separately. Figure 6a shows the TDOS image before and after doping Pd_3 cluster. After doping, the system curve moves to the direction of low energy level, indicating that the Pd_3 cluster doping reduces the band gap of GaSe. TDOS appeared a new peak near −0.6 eV, which may be caused by the hybridization of Pd and Se orbits. It can be perceived from the PDOS image in Figure 5b that Pd-4d orbital and Se-4p orbital are hybridized at the −0.6 eV, proving that Pd can form a stable chemical bond with Se and verifying the previous idea. Compared with the TDOS of Pd-GaSe system, the TDOS of Pd_3-GaSe system has a larger moving distance. Therefore, it is considered that the conductivity of GaSe system doped with Pd_3 cluster is improved more significantly than that of GaSe system doped with Pd. To sum up, it is speculated that Pd_3-GaSe system may have better gas adsorption.

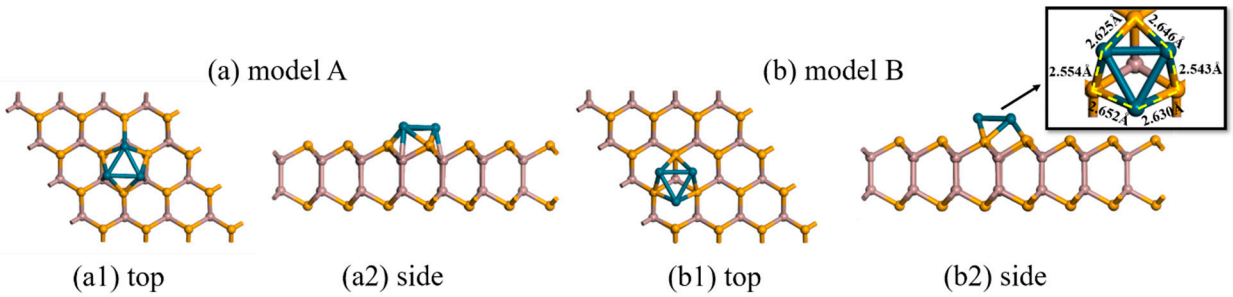


Figure 5. Two geometric models of Pd_3-GaSe monolayer.

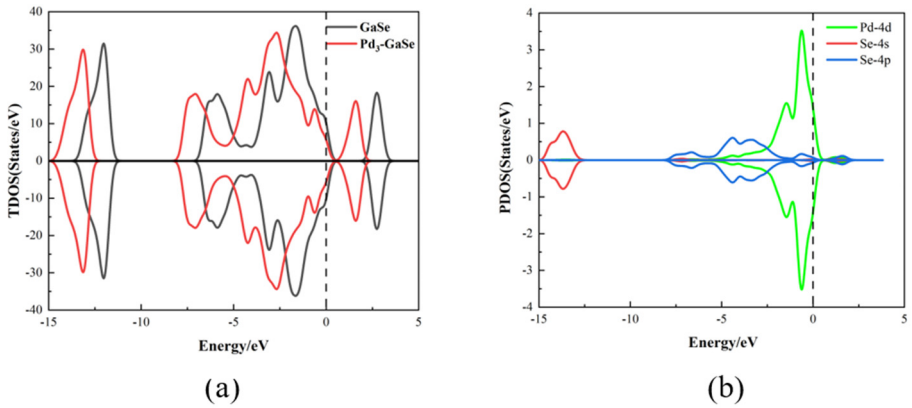


Figure 6. (**a**) TDOS of GaSe monolayer, Pd_3-GaSe monolayer, (**b**) PDOS of Pd_3-GaSe monolayer.

We consider all the adsorption sites for each gas, and build models to make gas molecules approach the adsorption materials in different ways. After geometric optimization, the adsorption energy of each adsorption model is calculated by Formula (2), and the models with the largest absolute value of adsorption energy are selected as the models for subsequent research.

3.2. H_2 Adsorption

The adsorption properties, charge transfer, and E_{ad} of H_2 on Pd-GaSe and Pd_3-Gase monolayers are shown in Figures 7 and 8, and Table 1. Some data of H_2 adsorption by intrinsic GaSe monolayer are also listed in Table 1. From the data in Table 1, the adsorption

energy of H_2 on GaSe monolayer is −0.544 eV, H_2 on Pd-GaSe monolayer is −0.58 eV, and H_2 on Pd_3-GaSe monolayer is −0.943 eV. It is worth noting that the adsorption distance of GaSe/H_2 system (3.504 Å) is almost twice that of Pd-GaSe/H_2 system (1.820 Å), but the adsorption energy of both systems is close. It can be noted that the Q_T of Pd-GaSe/H_2 system (0.108 e) is obviously more than that of GaSe/H_2 system (0.002 e), and the former has stronger charge transfer behavior. The results show that the doping of Pd improves the electronic behavior in the adsorption process, so the adsorption distance of Pd-GaSe/H_2 system is smaller than that of GaSe/H_2 system. However, from the point of view of adsorption energy, the two kinds of adsorption belong to weak physical adsorption, and the doping of Pd does not change the weak adsorption behavior of H_2. The doping method of Pd_3 cluster significantly enhances the system's adsorption performance for H_2, which belongs to chemical adsorption. Isolated H_2 has a bond length of 0.749 Å, and both kinds of doping make the H–H bond longer after adsorption. It can also be seen from the adsorption model that Pd_3-GaSe monolayer is obviously deformed during the adsorption process, and all three Pd atoms have shifted in different degrees. Pd cluster capture H_2, which indicates that there is a strong interaction between them. Mulliken atomic population analysis of H_2 molecule shows that 0.108 e electrons are transferred to Pd-GaSe monolayer and 0.199 e electrons are transferred to Pd_3-GaSe monolayer after H_2 adsorption. The results show that the doping method of Pd_3 cluster brings greater charge transfer amount than the doping method of Pd. Figures 7c and 8c show the deformation charge density (DCD) of the two adsorption systems. In the figure, red represents the charge accumulation zone and blue represents the charge depletion zone. In the two systems, there is an obvious blue area around Pd atom, which can be seen as the link of electron transfer between gas and material.

In Figure 7d, TDOS of the Pd-GaSe system shifted slightly to the right after H_2 adsorption, indicating that the electron orbit changed, but TDOS changed little during the adsorption process. The results indicate that H_2 has weak interaction with Pd-GaSe. TDOS shown in Figure 8d shows that after H_2 was adsorbed by Pd_3-GaSe system, TDOS decreased in the vicinity of −6.2 eV and increased significantly around −8.4 eV. In both systems, the spin-up and spin-down curves are symmetric, which means that the two H_2 adsorption systems are non-magnetic [57]. As shown in Figure 7e, in the Pd-GaSe system, slight hybridization exists between Pd-4d and H-1s orbitals near −7.3 eV and −0.1 eV. As shown in Figure 8e, in the Pd_3-GaSe system, the peak of H-1s orbital near −8.4 eV not only explains the increase of TDOS at −8.4 eV, but also indicates its hybridization with the Pd-4d orbital. Since the Pd-4d orbital overlaps with the H-1s orbital, it is speculated that a chemical bond may be formed between the two atoms. In conclusion, the doping method Pd_n (n is 1 or 3) can improve the H_2 adsorption performance of GaSe monolayer, and the H_2 adsorption performance of the Pd_3 cluster doping method is stronger than that of the Pd doping method.

Table 1. Adsorption characteristic parameters of H_2 adsorption.

Structure	The Length of Band (Å)		Adsorption Distance (Å)	Atom	Charge (e)	Q_T (e)	E_{ad} (eV)
GaSe/H_2	H_1-H_2	0.751	3.504	H_1 H_2	0.001 0.001	0.002	−0.544
Pd-GaSe/H_2	H_1-H_2	0.822	1.820	H_1 H_2 Pd	0.058 0.050 −0.249	0.108	−0.58
Pd_3-GaSe/H_2	H_1-H_2	0.847	1.726	H_1 H_2 Pd_1 Pd_2 Pd_3	0.100 0.099 −0.153 −0.336 −0.161	0.199	−0.943

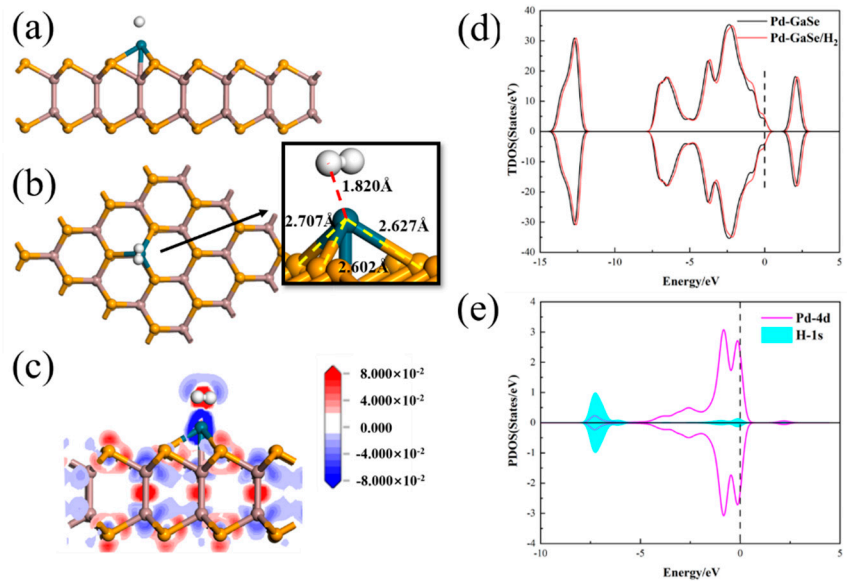


Figure 7. Adsorptive structure of Pd-GaSe/H_2 system (**a**) view of side, (**b**) view of top, (**c**) DCD distribution, (**d**) TDOS of Pd-GaSe/H_2 system, (**e**) PDOS of Pd-GaSe/H_2 system.

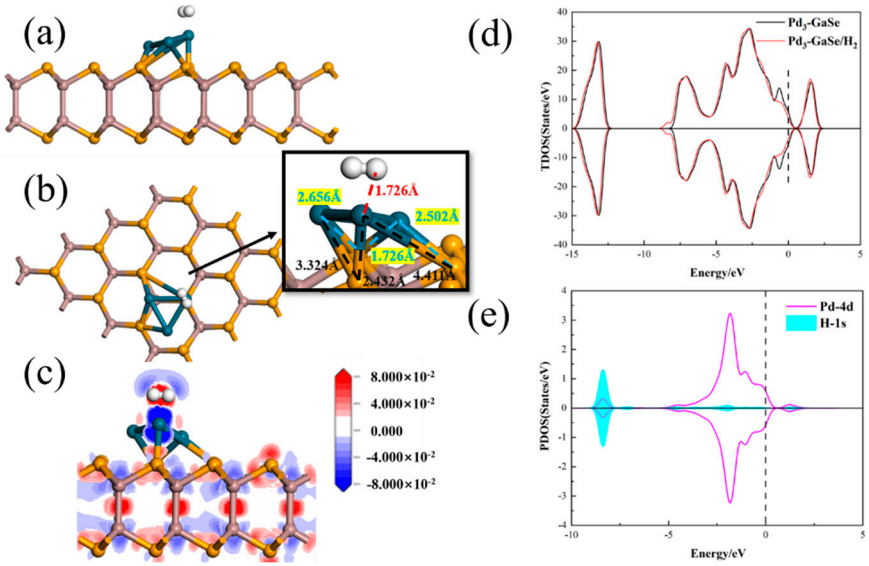


Figure 8. Adsorptive structure of Pd_3-GaSe/H_2 system (**a**) view of side, (**b**) view of top, (**c**) DCD distribution, (**d**) TDOS of Pd_3-GaSe/H_2 system, (**e**) PDOS of Pd_3-GaSe/H_2 system.

3.3. CO Adsorption

Parameters and structures related to CO adsorption are shown in Figures 9 and 10, and Table 2. From the data in Table 2, after CO adsorption, the adsorption energy of Pd-GaSe and Pd_3-GaSe systems are −1.587 eV and −2.427 eV respectively. When the absolute value of adsorption energy is greater than 0.8 eV, chemisorption exists. Therefore, the adsorption of CO by the two doped systems belongs to chemisorption. By comparing with the adsorption energy for CO of the intrinsic GaSe monolayer (−0.545 eV), indicating that the doping method of Pd_n (n is 1 or 3) obviously enhanced the adsorption of CO, and the enhanced adsorption effect may be caused by the formation of chemical bonds between CO and doping groups. In further proof, the length of C-O bond increased from 1.142 Å to 1.158 Å after adsorption on Pd-GaSe monolayer, while the length of C–O bond increased to 1.180 Å after adsorption on Pd_3-Gase monolayer. The change of bond length indicates that CO has certain activity in the adsorption process. In addition to the C–O bond, some Pd-Se

bonds in Pd_3-GaSe monolayer also increased obviously. Pd cluster capture CO molecules through C. Mulliken population analysis of CO molecule showed that 0.163 e electrons were transferred from CO molecule to Pd-GaSe monolayer after adsorption. After the adsorption of Pd_3-Gase monolayer, 0.187 e electrons were transferred from CO molecule to Pd_3-GaSe monolayer. In the DCD diagrams of Figures 9c and 10c, the blue area and the red area represent electron accumulation region and electron depletion region separately. As can be seen from the DCD diagrams of the two doping models, there is an obvious continuous electron region between Pd atom and CO gas molecule, which means that there is a strong chemical interaction between CO and the two adsorption materials.

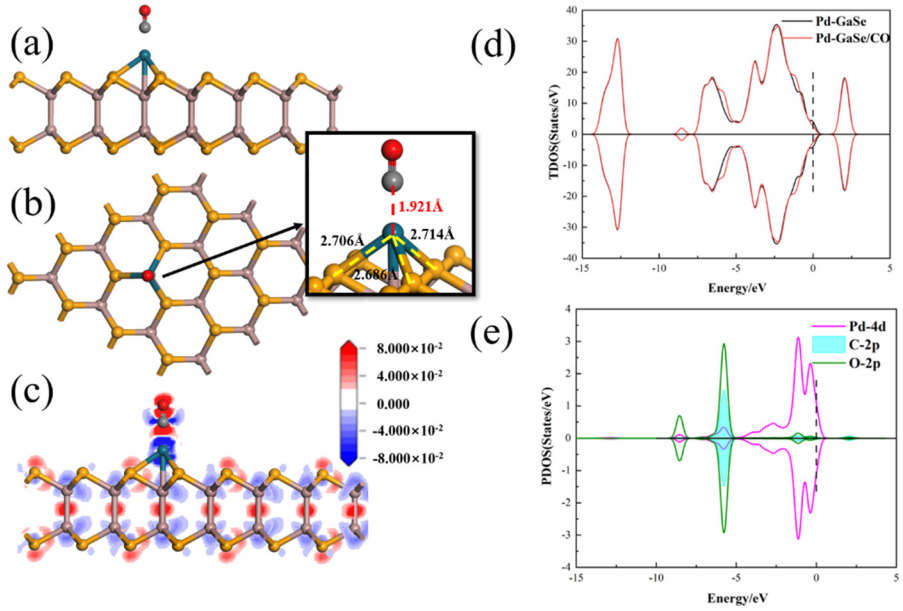


Figure 9. Adsorptive structure of Pd-GaSe/CO system (**a**) view of side, (**b**) view of top, (**c**) DCD distribution, (**d**) TDOS of Pd-GaSe/CO system, (**e**) PDOS of Pd-GaSe/CO system.

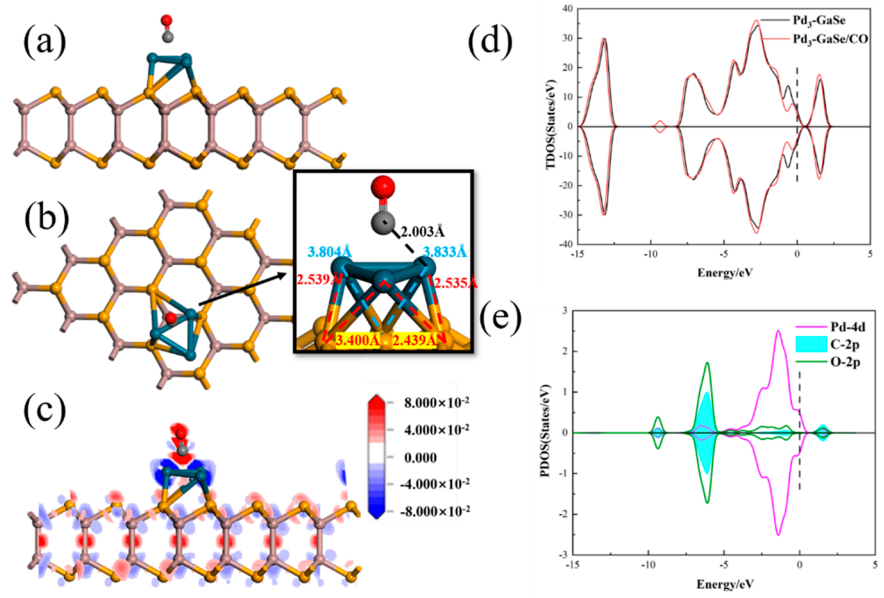


Figure 10. Adsorptive structure of Pd_3-GaSe/CO system (**a**) view of side, (**b**) view of top, (**c**) DCD distribution, (**d**) TDOS of Pd_3-GaSe/CO system, (**e**) PDOS of Pd_3-GaSe/CO system.

Table 2. Adsorption characteristic parameters of CO adsorption.

Structure	The Length of Bond (Å)		Adsorption Distance (Å)	Atom	Charge (e)	QT (e)	Ead (eV)
GaSe/CO	C-O	1.141	3.804	C O	0.111 −0.105	0.006	−0.545
Pd-GaSe/CO	C-O	1.158	1.921	C O Pd	0.307 −0.144 −0.334	0.163	−1.587
Pd_3-GaSe/CO	C-O	1.180	2.003	C O Pd_1 Pd_2 Pd_3	0.373 −0.186 −0.203 −0.206 −0.165	0.187	−2.427

Figure 9d,e show the DOS distribution of the Pd-GaSe system. After CO adsorption, the overall TDOS changes little and a new peak appears near −8.5 eV. The hybridization of the Pd-4d orbital, C-2p orbital, and O-2p orbital at −1.1 eV and −5.8 eV caused TDOS to rise around −1.1 eV and −5.8 eV. Figure 10d,e show the DOS distribution of the Pd_3-GaSe system. After adsorption, TDOS showed a new peak near −9.3 eV and decreased significantly at −0.6 eV. Pd-4d orbital, C-2p orbital, and O-2p orbital have overlapping regions around −0.9 eV and −6.1 eV, C-2p, and O-2p have obvious hybridization around 1.5 eV and −9.3 eV. These hybridization phenomena lead to changes in TDOS of the adsorption system, indicating that the adsorption of gas affects the electron behavior of Pd_3-GaSe monolayer. The results show that both Pd-GaSe monolayer and Pd_3-GaSe monolayer have an obvious adsorption effect on CO, and the adsorption performance of CO is significantly improved after doping Pd_n (n is 1 or 3). However, higher adsorption energy, higher charge transfer and more obvious gas molecules deformation show that Pd_3-Gase monolayer has better adsorption performance for CO.

3.4. C_2H_2 Adsorption

Figures 11 and 12, and Table 3 show the structures and related parameters of C_2H_2 adsorption. After the adsorption of C_2H_2 on the two doped materials, the structure of C_2H_2 has obvious deformation but still has good symmetry. In the Pd-GaSe/C_2H_2 system, H–C–C and C–C–H bond angles change to 155.279° and 155.552°, respectively. In the Pd_3-GaSe/C_2H_2 system, H–C–C and C–C–H bond angles decrease to 131.730° and 131.258°. As can be seen, in Pd_3-GaSe/C_2H_2 system, deformation of the C_2H_2 molecule is more severe, which may be related to the stronger reaction between adsorbent and C_2H_2. The adsorption energy of Pd-GaSe/C_2H_2 and Pd_3-GaSe/C_2H_2 systems are −1.307 eV and −2.757 eV, respectively, both of which belong to chemisorption. Compared with the direct adsorption of intrinsic GaSe monolayer (E_{ad} = −0.7 eV), the adsorption energy of the two doping systems for C_2H_2 were significantly increased, and the change of adsorption energy of Pd_3-GaSe/C_2H_2 system was particularly obvious, which also verified the previous conjecture. Moreover, from the adsorption model, it can be seen that Pd_3-GaSe has a strong adsorption effect on C_2H_2. After adsorption, three Pd atoms shift obviously and capture C_2H_2, but the monolayer of Pd-GaSe does not change obviously. In the Pd-GaSe/C_2H_2 system, Pd atom carries 0.296 e electrons after C_2H_2 molecule transfers 0.1 e electrons to Pd-GaSe monolayer, indicating that Pd atom obtains electrons from GaSe monolayer. Similarly, Pd acts as an electron acceptor in the Pd_3-GaSe/C_2H_2 system, accepting electrons from gas molecules and GaSe monolayer. As can be seen from the DCD diagrams in Figures11c and 12c, the overlap between the red and blue areas between the gas and the material indicates a large amount of electron transfer and strong chemical reaction strength.

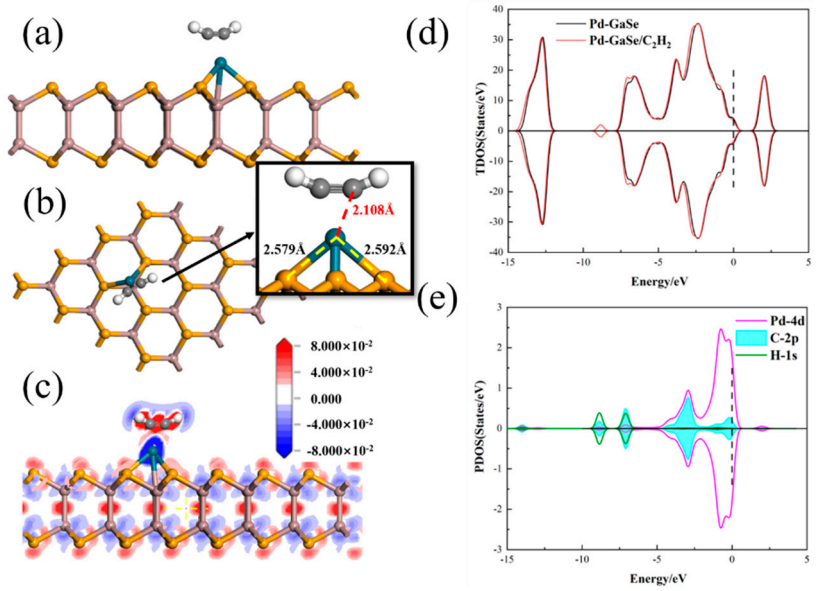


Figure 11. Adsorptive structure of Pd-GaSe/C_2H_2 system (**a**) view of side, (**b**) view of top, (**c**) DCD distribution, (**d**) TDOS of Pd-GaSe/C_2H_2 system, (**e**) PDOS of Pd-GaSe/C_2H_2 system.

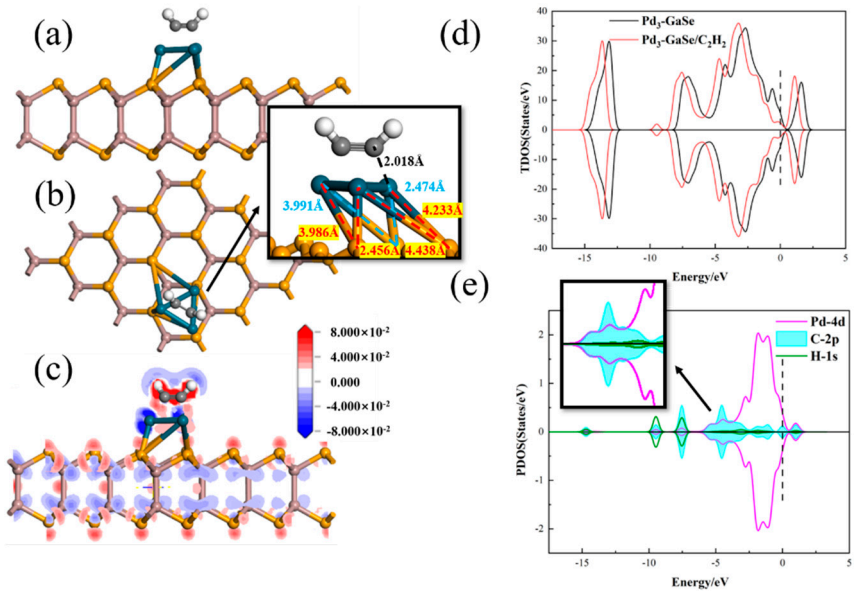


Figure 12. Adsorptive structure of Pd_3-GaSe/C_2H_2 system (**a**) view of side, (**b**) view of top, (**c**) DCD distribution, (**d**) TDOS of Pd_3-GaSe/ C_2H_2 system, (**e**) PDOS of Pd_3-GaSe/ C_2H_2 system.

DOS distribution of Pd-GaSe/C_2H_2 system is shown in Figure 11d,e. After adsorption of C_2H_2, the TDOS of the system appeared a new peak near −8.8 eV, but there was no obvious change. In addition, the Pd-4d orbital and C-2p orbital overlap at −0.1 eV, −2.9 eV, and −7.1 eV, and hybridization between orbitals causes strong orbital interactions. Based on the TDOS distribution of the Pd_3-GaSe/C_2H_2 system shown in Figure 12d, the overall TDOS shifted significantly to the left after adsorption, indicating that its electrical conductivity was significantly enhanced. As can be seen from the PDOS distribution in Figure 12e, obvious orbital hybridization exists in Pd-4d and C-2p orbitals at 0.1 eV, −1.1 eV, −4.5 eV, and −7.5 eV. It means that chemical bonds are formed between Pd atom and C atom. From the above analysis, it can be seen that Pd_3-GaSe monolayer shows strong adsorption of C_2H_2. In conclusion, after Pd_n (n is 1 or 3) doping, the adsorption performance of the system for C_2H_2 is significantly enhanced, and various data show that

Pd_3 cluster doped with GaSe monolayer have better adsorption performance of C_2H_2 than Pd-GaSe system.

Table 3. Adsorption characteristic parameters of C_2H_2 adsorption.

Structure	The Length of Bond (Å)		Bond Angle (°)		Adsorption Distance (Å)	Atom	Charge (e)	Q_T (e)	E_{ad} (eV)
GaSe/C_2H_2	C_1-C_2	1.212	H_1-C_1-C_2	179.704	3.593	C_1	−0.123	0.004	−0.700
						C_2	−0.127		
	C_1-H_1	1.072	C_1-C_2-H_2	179.283		H_1	0.126		
	C_2-H_2	1.072				H_2	0.128		
Pd-GaSe/C_2H_2	C_1-C_2	1.261	H_1-C_1-C_2	155.279	2.108	C_1	−0.062	0.100	−1.307
						C_2	−0.060		
	C_1-H_1	1.079	C_1-C_2-H_2	155.552		H_1	0.111		
						H_2	0.111		
	C_2-H_2	1.079				Pd	−0.296		
Pd_3-GaSe/C_2H_2	C_1-C_2	1.337	H_1-C_1-C_2	131.730	2.018	C_1	−0.026	0.178	−2.757
						C_2	−0.035		
						H_1	0.119		
	C_1-H_1	1.097	C_1-C_2-H_2	131.258		H_2	0.120		
						Pd_1	−0.212		
	C_2-H_2	1.096				Pd_2	−0.204		
						Pd_3	−0.208		

3.5. Frontier Orbital Theory Analysis

To further elucidate the changes in the conductivity of Pd-GaSe and Pd_3-GaSe monolayers caused by gas adsorption, the lowest unoccupied molecular orbital (LUMO) and highest occupied molecular orbital (HOMO) were calculated according to the frontier molecular orbital (FMO) theory. The relationship between band gap and conductivity is shown as follows:

$$\sigma \propto \exp(-E_g / 2k_BT) \quad (4)$$

where k_B and T represent Boltzmann constant and temperature respectively. According to the formula, the narrower the band gap means that it has greater conductivity when the temperature is constant. Thus, the narrower the band gap, the easier the electron transfer.

Refer to Figure 13a, LUMO and HOMO are mostly distributed around Pd atoms in the Pd-GaSe system. After gas molecule adsorption, LUMO and HOMO distribution of the Pd-GaSe/H_2 system does not change much compared with that before adsorption, meaning that the interaction force between gas and adsorption material is weak after H_2 adsorption. In Pd-GaSe/CO and Pd-GaSe/C_2H_2 systems, LUMO is mainly distributed in Pd-GaSe monolayer, HOMO is mainly distributed in the vicinity of gas molecules and Pd atoms. After the adsorption of the three gas molecules, the band gaps of the adsorption systems all increase, indicating that the conductivity of the adsorption systems decreases after gas adsorption. Since the band gap increase of Pd-GaSe/C_2H_2 system is not obvious, the sensitivity of the sensor to C_2H_2 detection is limited. Therefore, Pd-GaSe can be used as a semiconductor sensor to detect H_2 and CO.

In Figure 13b, before gas adsorption, LUMO and HOMO are mainly distributed around the Pd_3 group before gas adsorption, which indicated that there is a high electron concentration in the vicinity of the Pd_3 cluster. After gas adsorption, HOMO of the system is mainly distributed near gas molecules and Pd_3 cluster. Except for the Pd_3-GaSe/H_2 system, the LUMO of the other two systems is rarely distributed near the gas and Pd_3 cluster. Compared with Pd_3-GaSe, the band gap of Pd_3-GaSe/C_2H_2 system decreased significantly, indicating that the electrical conductivity increased significantly after adsorption. However, the band gaps of Pd_3-GaSe/H_2 and Pd_3-GaSe/CO systems increased and the conductivity decreased after gas adsorption. Therefore, Pd_3-GaSe can be used as a sensor material to detect these three gases.

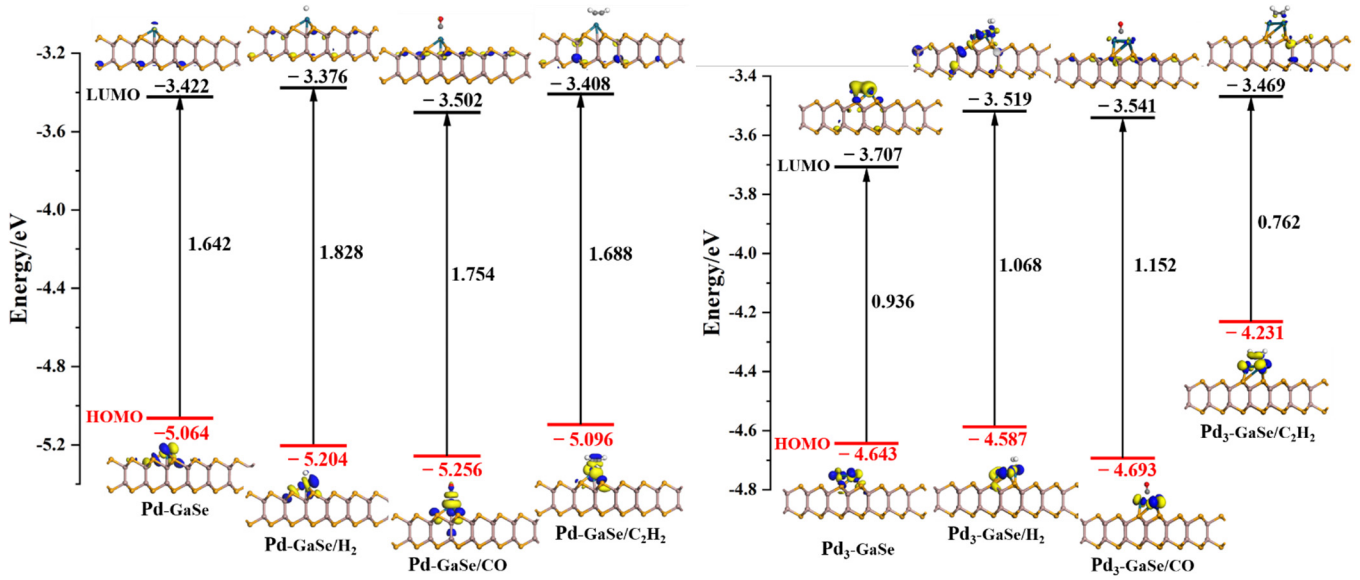


Figure 13. HOMO and LUMO distributions of (**a**) Pd-GaSe adsorption system and (**b**) Pd_3-GaSe adsorption system.

3.6. Analysis of Recovery Time

As an important index, recovery time is used to indicate the desorption capacity of gas-sensitive materials to characteristic gases, which can be obtained by the following equation:

$$\tau = A^{-1}e^{(-E_a/K_BT)} \quad (5)$$

In the above formula, A and T represent the attempt frequency and temperature, A is constant and equal to 10^{12} s^{-1}. [30,58,59] K_B represents Boltzmann constant (8.62×10^{-5} eV/K). E_a represents the energy to be overcome in the desorption process, and its value can be considered to be equal to E_{ad}. Figure 14 shows the recovery time of the three gas molecules on the Pd-GaSe and Pd_3-GaSe systems at 298 K, 398 K, and 498 K. The recovery time of H_2 in Pd-GaSe is very short, and the adsorptive H_2 will soon break away from the binding of the material, indicating that Pd-GaSe is not suitable as H_2 scavenger. When the temperature is 398 K, the recovery time of H_2 on Pd_3-GaSe is 0.87 s, and when the temperature is 298 K, the recovery time is 8780 s (2.4 h), meaning that Pd_3-GaSe is an ideal gas sensitive material for the detection of H_2. CO is difficult to desorption on the two adsorption systems at three temperatures, which means that there is a strong interaction between adsorbent and gas molecule. Therefore, both doping structures can be used as disposable CO scavengers. At 298 K, C_2H_2 is difficult to desorption from Pd-GaSe monolayer, but the recovery time is 16.7 s when the temperature rises to 498 K. Pd-GaSe has a strong adsorption of C_2H_2 at room temperature, and the recovery time is very short at high temperature. However, after adsorption of C_2H_2, the increase of conductivity is not obvious. Therefore Pd-GaSe is more suitable as a reusable C_2H_2 scavenger than for detecting C_2H_2. However, the desorption time of C_2H_2 on Pd_3-GaSe is very long, and Pd_3-GaSe can be used as a one-time scavenger of C_2H_2.

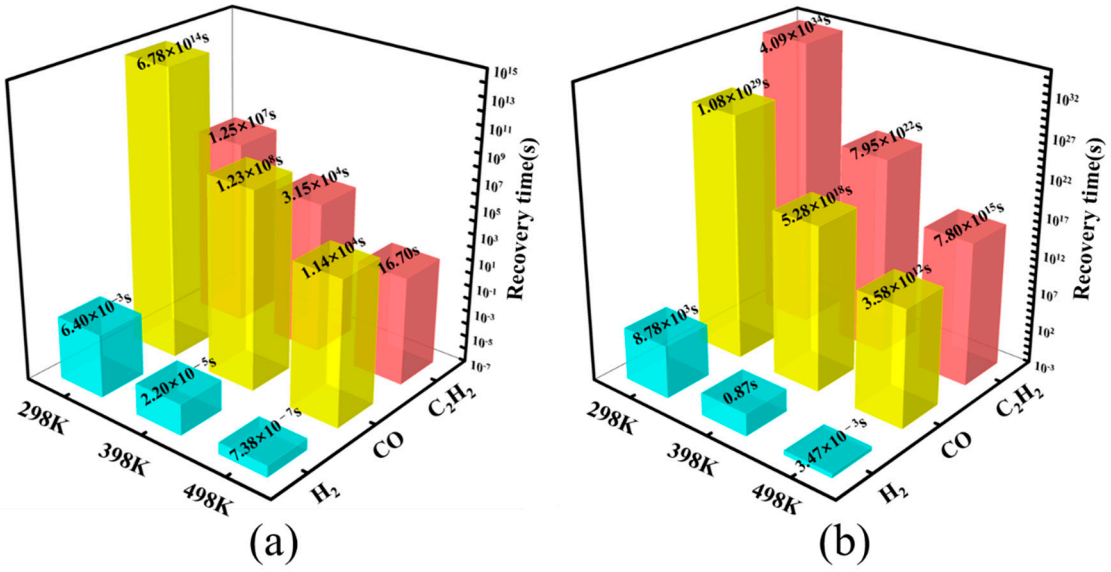


Figure 14. Recovery time of (**a**) Pd-GaSe adsorption system and (**b**) Pd_3-GaSe adsorption system.

4. Conclusions

In this study, the adsorption behaviors of Pd-GaSe and Pd_3-GaSe monolayers on three gases (H_2, CO, and C_2H_2) decomposed by the transformer oil were studied using DFT calculations. The results show that Pd mono-atom doping and Pd_3 cluster doping can improve the adsorption capacity of the materials to the three gases compared with the intrinsic GaSe monolayer. The adsorption performance of Pd_3-GaSe for three gases is better than that of Pd-GaSe. All three kinds of adsorption of Pd_3-GaSe are chemical adsorption. It is speculated that the increase in the number of doped Pd atoms changes the original structure and charge distribution to a greater extent, more obviously enhances the conductivity, and thus enhances the adsorption performance of the gas. Through the analysis of DOS, the above viewpoint is also proved. By analyzing the frontier molecular orbitals and recovery characteristics, Pd_3-GaSe can be used as an ideal gas sensitive material for H_2 detection because of its good desorption properties and obvious conductivity changes. Pd-GaSe can also be used as a disposable resistive sensor for CO. Pd_3-GaSe is a sensing material suitable for the disposable resistive sensor for CO and C_2H_2. Therefore, Pd-GaSe and Pd_3-GaSe monolayers have great application potential in gas detection and adsorption, and are of important significance to the safe operation of power equipment.

Author Contributions: Conceptualization, T.H.; methodology, T.H. and Q.Z.; validation, T.H. and Q.Z.; investigation, T.H.; resources, Q.Z.; data curation, T.H.; writing—original draft preparation review and editing, T.H.; writing—review and editing, T.H., Q.Z. and W.Z.; visualization, T.H.; supervision, Q.Z.; project administration, Q.Z. and W.Z. All authors have read and agreed to the published version of the manuscript.

Funding: This study has been supported in part of by the National Natural Science Foundation of China (Nos. 52077177 and 51507144) and Fundamental Research Funds for the Central Universities (No. XDJK2019B021).

Institutional Review Board Statement: Not applicable.

Informed Consent Statement: Not applicable.

Data Availability Statement: The data is available on the request from corresponding author.

Conflicts of Interest: The authors declare no conflict of interest.

References

1. Tenbohlen, S.; Coenen, S.; Djamali, M.; Muller, A.; Samimi, M.H.; Siegel, M. Diagnostic Measurements for Power Transformers. *Energies* **2016**, *9*, 347. [CrossRef]
2. Wang, J.C.; Zhang, X.X.; Liu, L.; Wang, Z.T. Dissolved gas analysis in transformer oil using Ni-Doped GaN monolayer: A DFT study. *Superlattices Microstruct.* **2021**, *159*, 107055. [CrossRef]
3. Alsuhaibani, S.; Khan, Y.; Beroual, A.; Malik, N.H. A Review of Frequency Response Analysis Methods for Power Transformer Diagnostics. *Energies* **2016**, *9*, 879. [CrossRef]
4. Bustamante, S.; Manana, M.; Arroyo, A.; Castro, P.; Laso, A.; Martinez, R. Dissolved Gas Analysis Equipment for Online Monitoring of Transformer Oil: A Review. *Sensors* **2019**, *19*, 4057. [CrossRef] [PubMed]
5. He, X.; Gui, Y.G.; Xie, J.F.; Liu, X.; Wang, Q.; Tang, C. A DFT study of dissolved gas (C_2H_2, H_2, CH_4) detection in oil on CuO-modified BNNT. *Appl. Surf. Sci.* **2020**, *500*, 144030. [CrossRef]
6. Singh, S.; Bandyopadhyay, M.N. Dissolved Gas Analysis Technique for Incipient Fault Diagnosis in Power Transformers: A Bibliographic Survey. *IEEE Electr. Insul. Mag.* **2010**, *26*, 41–46. [CrossRef]
7. Yang, X.; Wu, X.; Li, J. Recent advances in screening two-dimensional materials for high-performance energy storage and conversion devices based on electronic structure theory. *Chin. Sci. Bull. Chin.* **2021**, *66*, 640–656. [CrossRef]
8. Zhou, Z.X.; Yap, Y.K. Two-Dimensional Electronics and Optoelectronics: Present and Future. *Electronics* **2017**, *6*, 53. [CrossRef]
9. Bag, A.; Lee, N.E. Gas sensing with heterostructures based on two-dimensional nanostructured materials: A review. *J. Mater. Chem. C* **2019**, *7*, 13367–13383. [CrossRef]
10. Chaudhari, N.K.; Jin, H.; Kim, B.; Baek, D.S.; Joo, S.H.; Lee, K. MXene: An emerging two-dimensional material for future energy conversion and storage applications. *J. Mater. Chem. A* **2017**, *5*, 24564–24579. [CrossRef]
11. Bao, J.; Jeppson, K.; Edwards, M.; Fu, Y.F.; Ye, L.L.; Lu, X.Z.; Liu, J. Synthesis and Applications of Two-Dimensional Hexagonal Boron Nitride in Electronics Manufacturing. *Electron. Mater. Lett.* **2016**, *12*, 1–16. [CrossRef]
12. Yang, T.; Cui, Y.N.; Chen, H.Y.; Li, W.H. Controllable Preparation of Two Dimensional Metal- or Covalent Organic Frameworks for Chemical Sensing and Biosensing. *Acta Chim. Sin.* **2017**, *75*, 339–350. [CrossRef]
13. Abu Bakar, N.; Abu-Siada, A.; Islam, S. A Review of Dissolved Gas Analysis Measurement and Interpretation Techniques. *IEEE Electr. Insul. Mag.* **2014**, *30*, 39–49. [CrossRef]
14. Cilliyuz, Y.; Bicen, Y.; Aras, F.; Aydugan, G. Measurements and performance evaluations of natural ester and mineral oil-immersed identical transformers. *Int. J. Electr. Power Energy Syst.* **2021**, *125*, 106517. [CrossRef]
15. Faiz, J.; Soleimani, M. Dissolved Gas Analysis Evaluation in Electric Power Transformers using Conventional Methods a Review. *IEEE Trans. Dielectr. Electr. Insul.* **2017**, *24*, 1239–1248. [CrossRef]
16. Kondalkar, V.V.; Park, J.; Lee, K. MEMS hydrogen gas sensor for in-situ monitoring of hydrogen gas in transformer oil. *Sens. Actuators* B Chem. **2021**, *326*, 128989. [CrossRef]
17. Qian, G.C.; Peng, Q.J.; Zou, D.X.; Wang, S.; Yan, B.; Zhou, Q. First-Principles Insight into Au-Doped MoS_2 for Sensing C_2H_6 and C_2H_4. *Front. Mater.* **2020**, *7*, 22. [CrossRef]
18. Rezaie, S.; Bafghi, Z.G.; Manavizadeh, N.; Kordmahale, S.B. Highly Sensitive Detection of Dissolved Gases in Transformer Oil with Carbon-Doped ZnO Nanotube: A DFT Study. *IEEE Sens. J.* **2022**, *22*, 82–89. [CrossRef]
19. Mi, H.W.; Zhou, Q.; Zeng, W. A density functional theory study of the adsorption of Cl_2, NH_3, and NO_2 on Ag_3-doped WSe_2 monolayers. *Appl. Surf. Sci.* **2021**, *563*, 150329. [CrossRef]
20. Yuan, T.; Fu, C.; Gong, Y.J.; Tong, Y.; Zhang, J.; Wang, Y.Q. First-principles Insights into Cu-Decorated GaN Monolayers for Sensing CO and HCHO in Dry-Type Transformers. *ACS Omega* **2021**, *6*, 19127–19133. [CrossRef]
21. Hu, P.A.; Wen, Z.Z.; Wang, L.F.; Tan, P.H.; Xiao, K. Synthesis of Few-Layer GaSe Nanosheets for High Performance Photodetectors. *ACS Nano* **2012**, *6*, 5988–5994. [CrossRef]
22. Late, D.J.; Liu, B.; Luo, J.J.; Yan, A.M.; Matte, H.; Grayson, M.; Rao, C.N.R.; Dravid, V.P. GaS and GaSe Ultrathin Layer Transistors. *Adv. Mater.* **2012**, *24*, 3549–3554. [CrossRef]
23. Zhuang, H.L.L.; Hennig, R.G. Single-Layer Group-III Monochalcogenide Photocatalysts for Water Splitting. *Chem. Mater.* **2013**, *25*, 3232–3238. [CrossRef]
24. Jie, W.J.; Chen, X.; Li, D.; Xie, L.; Hui, Y.Y.; Lau, S.P.; Cui, X.D.; Hao, J.H. Layer-Dependent Nonlinear Optical Properties and Stability of Non-Centrosymmetric Modification in Few-Layer GaSe Sheets. *Angew. Chem. Int. Ed.* **2015**, *54*, 1185–1189. [CrossRef]
25. Zhou, C.J.; Zhu, H.L.; Wu, Y.P.; Lin, W.; Yang, W.H.; Dong, L.X. Effect of external strain on the charge transfer: Adsorption of gas molecules on monolayer GaSe. *Mater. Chem. Phys.* **2017**, *198*, 49–56. [CrossRef]
26. Chen, D.C.; Zhang, X.X.; Tang, J.; Cui, H.; Li, Y. Noble metal (Pt or Au)-doped monolayer MoS_2 as a promising adsorbent and gas-sensing material to SO_2, SOF_2 and SO_2F_2: A DFT study. *Appl. Phys. A* **2018**, *124*, 194. [CrossRef]
27. Chen, G.X.; Li, H.F.; Wang, D.D.; Li, S.Q.; Fan, X.B.; Zhang, J.M. Adsorption of toxic gas molecules on pristine and transition metal doped hexagonal GaN monolayer: A first-principles study. *Vacuum* **2019**, *165*, 35–45. [CrossRef]
28. Ni, J.M.; Quintana, M.; Song, S.X. Adsorption of small gas molecules on transition metal (Fe, Ni and Co, Cu) doped graphene: A systematic DFT study. *Phys. E Low-Dimens. Syst. Nanostruct.* **2020**, *116*, 113768. [CrossRef]
29. Jiang, T.Y.; Zhang, T.; He, Q.Q.; Bi, M.Q.; Chen, X.; Zhou, X. Adsorption performance and gas-sensing properties of V-GaSe to SF_6 decomposition components in gas-insulated switchgear. *Appl. Surf. Sci.* **2022**, *577*, 151854. [CrossRef]

30. Cui, H.; Zhang, X.X.; Zhang, G.Z.; Tang, J. Pd-doped MoS_2 monolayer: A promising candidate for DGA in transformer oil based on DFT method. *Appl. Surf. Sci.* **2019**, *470*, 1035–1042. [CrossRef]
31. Ma, L.; Zhang, J.M.; Xu, K.W.; Ji, V. A first-principles study on gas sensing properties of graphene and Pd-doped graphene. *Appl. Surf. Sci.* **2015**, *343*, 121–127. [CrossRef]
32. Cui, H.; Jia, P.F.; Peng, X.Y. Adsorption of SO_2 and NO_2 molecule on intrinsic and Pd-doped $HfSe_2$ monolayer: A first-principles study. *Appl. Surf. Sci.* **2020**, *513*, 145863. [CrossRef]
33. Gao, Z.Y.; Li, A.; Liu, X.S.; Ma, C.Z.; Li, X.; Yang, W.J.; Ding, X.L. Density functional study of the adsorption of NO on Ni-n (n=1, 2, 3 and 4) clusters doped functionalized graphene support. *Appl. Surf. Sci.* **2019**, *481*, 940–950. [CrossRef]
34. Cui, H.; Jia, P.F. Doping effect of small Rh_n (n = 1–4) clusters on the geometric and electronic behaviors of MoS_2 monolayer: A first-principles study. *Appl. Surf. Sci.* **2020**, *526*, 146659. [CrossRef]
35. Delley, B. From molecules to solids with the $DMol^3$ approach. *J. Chem. Phys.* **2000**, *113*, 7756–7764. [CrossRef]
36. Lee, S.G.; Choi, J.I.; Koh, W.; Jang, S.S. Adsorption of beta-D-glucose and cellobiose on kaolinite surfaces: Density functional theory (DFT) approach. *Appl. Clay Sci.* **2013**, *71*, 73–81. [CrossRef]
37. Tkatchenko, A.; DiStasio, R.A.; Head-Gordon, M.; Scheffler, M. Dispersion-corrected Moller-Plesset second-order perturbation theory. *J. Chem. Phys.* **2009**, *131*, 094106. [CrossRef]
38. Zeng, F.P.; Feng, X.X.; Chen, X.Y.; Yao, Q.; Miao, Y.L.; Dai, L.J.; Li, Y.; Tang, J. First-principles analysis of $Ti_3C_2T_x$ MXene as a promising candidate for SF_6 decomposition characteristic components sensor. *Appl. Surf. Sci.* **2022**, *578*, 152020. [CrossRef]
39. Cui, H.; Zhang, X.X.; Chen, D.C.; Tang, J. Adsorption mechanism of SF6 decomposed species on pyridine-like PtN_3 embedded CNT: A DFT study. *Appl. Surf. Sci.* **2018**, *447*, 594–598. [CrossRef]
40. Gao, X.; Zhou, Q.; Wang, J.X.; Xu, L.N.; Zeng, W. DFT Study on the Selective Adsorption Properties of Modified Graphene for SF_6 Decompositions. *IEEE Sens. J.* **2021**, *21*, 3193–3200. [CrossRef]
41. Pakornchote, T.; Ektarawong, A.; Alling, B.; Pinsook, U.; Tancharakorn, S.; Busayaporn, W.; Bovornratanaraks, T. Phase stabilities and vibrational analysis of hydrogenated diamondized bilayer graphenes: A first principles investigation. *Carbon* **2019**, *146*, 468–475. [CrossRef]
42. Monkhorst, H.J.; Pack, J.D. Special points for Brillouin-zone integrations. *Phys. Rev. B* **1976**, *13*, 5188. [CrossRef]
43. Mom, R.V.; Cheng, J.; Koper, M.T.M.; Sprik, M. Modeling the Oxygen Evolution Reaction on Metal Oxides: The Infuence of Unrestricted DFT Calculations. *J. Phys. Chem. C* **2014**, *118*, 4095–4102. [CrossRef]
44. Li, B.L.; Zhou, Q.; Peng, R.C.; Liao, Y.M.; Zeng, W. Adsorption of SF6 decomposition gases (H_2S, SO_2, SOF_2 and SO_2F_2) on Sc-doped MoS_2 surface: A DFT study. *Appl. Surf. Sci.* **2021**, *549*, 149271.
45. Zhang, X.X.; Wang, J.C.; Chen, D.C.; Liu, L. The adsorption performance of harmful gas on Cu doped WS_2: A first-principle study. *Mater. Today Commun.* **2021**, *28*, 102488. [CrossRef]
46. Chen, D.C.; Li, Y.; Xiao, S.; Yang, C.X.; Zhou, J.; Xiao, B.B. Single Ni atom doped WS_2 monolayer as sensing substrate for dissolved gases in transformer oil: A first-principles study. *Appl. Surf. Sci.* **2022**, *579*, 152141. [CrossRef]
47. Zhang, X.X.; Cui, H.; Zhang, J.; Tang, J. Adsorption characteristic of Pd-4 cluster carbon nanotube towards transformer oil dissolved components: A simulation. *Appl. Surf. Sci.* **2017**, *419*, 802–810. [CrossRef]
48. Xiao, Z.; Wu, W.; Wu, X.W.; Zhang, Y.F. Adsorption of NO_2 on monolayer MoS_2 doped with Fe, Co, and Ni, Cu: A computational investigation. *Chem. Phys. Lett.* **2020**, *755*, 137768. [CrossRef]
49. Ye, X.; Jiang, X.; Chen, L.; Jiang, W.J.; Wang, H.L.; Cen, W.L.; Ma, S.G. Effect of manganese dioxide crystal structure on adsorption of SO_2 by DFT and experimental study. *Appl. Surf. Sci.* **2020**, *521*, 146477. [CrossRef]
50. Cui, H.; Guo, Y.X.; Zhao, Q.; Zhang, G.Z. Pd-doped $PtSe_2$ monolayer with strain-modulated effect for sensing SF_6 decomposed species: A first-principles study. *J. Mater. Res. Technol.* **2022**, *18*, 629–636. [CrossRef]
51. Gui, X.X.; Zhou, Q.; Peng, S.D.; Xu, L.N.; Zeng, W. Adsorption behavior of Rh -doped MoS_2 monolayer towards SO_2, SOF_2, SO_2F_2 based on DFT study. *Phys. E Low-Dimens. Syst. Nanostruct.* **2020**, *122*, 114224. [CrossRef]
52. Zhang, X.X.; Cui, H.; Dong, X.C.; Chen, D.C.; Tang, J. Adsorption performance of Rh decorated SWCNT upon SF_6 decomposed components based on DFT method. *Appl. Surf. Sci.* **2017**, *420*, 825–832. [CrossRef]
53. Liu, D.K.; Gui, Y.G.; Ji, C.; Tang, C.; Zhou, Q.; Li, J.; Zhang, X.X. Adsorption of SF_6 decomposition components over Pd (111): A density functional theory study. *Appl. Surf. Sci.* **2019**, *465*, 172–179. [CrossRef]
54. Gui, X.X.; Zhou, Q.; Peng, S.D.; Xu, L.N.; Zeng, W. Dissolved gas analysis in transformer oil using Sb-doped graphene: A DFT study. *Appl. Surf. Sci.* **2020**, *533*, 147509. [CrossRef]
55. Liu, Y.P.; Zhou, Q.; Hou, W.J.; Li, J.; Zeng, W. Adsorption properties of Cr modified GaN monolayer for H_2, CO, C_2H_2 and C_2H_4. *Chem. Phys.* **2021**, *550*, 111304. [CrossRef]
56. Liao, Y.M.; Zhou, Q.; Hou, W.J.; Li, J.; Zeng, W. Theoretical study of dissolved gas molecules in transformer oil adsorbed on intrinsic and Cr-doped InP_3 monolayer. *Appl. Surf. Sci.* **2021**, *561*, 149816. [CrossRef]
57. Li, Z.H.; Jia, L.F.; Chen, J.X.; Cui, X.S.; Zeng, W.; Zhou, Q. Ag-modified hexagonal GaN monolayer as an innovative gas detector toward SF_6 decomposed species: Insights from the first-principles computations. *Appl. Surf. Sci.* **2022**, *589*, 153000. [CrossRef]
58. Boerner, E.D.; Bertram, H.N. Non-Arrhenius behavior in single domain particles. *IEEE Trans. Magn.* **1998**, *34*, 1678–1680. [CrossRef]
59. Lee, J.M.; Lim, S.H. Thermally activated magnetization switching in a nanostructured synthetic ferrimagnet. *J. Appl. Phys.* **2013**, *113*, 063914.